

IL NUOVO CIMENTO
DOI 10.1393/ncc/i2010-10574-4

VOL. 33 C, N. 1

Gennaio-Febbraio 2010

COLLOQUIA: ICTT2009

Parallel algorithms for simulation of ultrashort pulse propagation in turbid media

L. P. BASS^{(1)(*)}, O. V. NIKOLAEVA^{(1)(**)}, V. S. KUZNETSOV^{(2)(***)},
A. V. BYKOV^{(3)(4)(**)} and A. V. PRIEZZHEV^{(3)(**)}

⁽¹⁾ *Keldysh Institute of Applied Mathematics - Moscow, Russia*

⁽²⁾ *Research Center "Kurchatov Institute" - Moscow, Russia*

⁽³⁾ *Lomonosov Moscow State University - Moscow, Russia*

⁽⁴⁾ *University of Oulu - Oulu, Finland*

(ricevuto il 30 Ottobre 2009; approvato il 25 Gennaio 2010; pubblicato online il 9 Marzo 2010)

Summary. — Parallel mesh algorithm to simulate the propagation of an ultrashort pulse from a point source with small aperture in turbid media is presented. The algorithm is applied to a particular case of propagation of infrared pulsed laser radiation in biotissue. Comparison of obtained results with Monte Carlo simulation ones is performed.

PACS 42.25.Bs – Wave propagation, transmission and absorption.

PACS 42.62.Be – Biological and medical applications.

Introduction

Simulation of interaction of ultrashort light pulses and turbid media has an important part in solving many problems of mathematical and optical physics. Fast algorithms are in great demand because solving inverse problems of retrieval of media properties via registered responses is usually performed via repeated direct calculations. Commonly used Monte Carlo simulations take too much time and are not free of statistical noise. Thus designing alternative computation techniques that would require less computation time and have no inherent statistical noise is a hot problem.

(*) E-mail: bass@kiam.ru

(**) E-mail: nika@kiam.ru

(***) E-mail: lri@bk.ru

(**) E-mail: sasha5000@tut.by

(**) E-mail: avp2@mail.ru

Mesh algorithms of the discrete ordinate method aimed at the solution of the radiative transfer equation potentially allow faster calculations than the Monte Carlo technique. Besides, mesh solutions are not distorted by statistical noise. However mesh algorithms are more difficult for implementation than Monte Carlo ones and, therefore, seldomly used.

In this work, we present a new mesh algorithm. It is based upon analytical calculation of the unscattered and single-scattered radiation intensity, a mesh scheme to calculate the multiple-scattered radiation intensity and parallel computations to reduce the calculation time.

The paper is organized as follows. The non-stationary transport problem with a pulsed point source with small aperture is formulated in sect. 1. Mesh method to this problem is outlined in sect. 2. Special approaches to reduce the calculation time are described in sect. 3. Numerical results are presented in sect. 4.

1. – Mathematical problem

We consider the non-stationary radiation transfer equation

$$(1.1) \quad \begin{aligned} (1/v)\partial\Psi/\partial t + \hat{L}\Psi(\mathbf{r}, \mathbf{\Omega}, t) &= \hat{S}\Psi(\mathbf{r}, \mathbf{\Omega}, t) + Q(\mathbf{r}, \mathbf{\Omega}, t), \quad \mathbf{r} \in G, \\ \hat{L}\Psi(\mathbf{r}, \mathbf{\Omega}, t) &= \mathbf{\Omega} \cdot \nabla \Psi(\mathbf{r}, \mathbf{\Omega}, t) + \Sigma_t(\mathbf{r})\Psi(\mathbf{r}, \mathbf{\Omega}, t), \\ \hat{S}\Psi(\mathbf{r}, \mathbf{\Omega}, t) &= \Sigma_S(\mathbf{r}) \int_{\Omega} p(\mathbf{r}, \mathbf{\Omega}, \mathbf{\Omega}')\Psi(\mathbf{r}, \mathbf{\Omega}', t) d\mathbf{\Omega}'. \end{aligned}$$

Here, the solution $\Psi(\mathbf{r}, \mathbf{\Omega}, t)$ is the radiation intensity at the spatial point \mathbf{r} of the region G in the direction of unit vector $\mathbf{\Omega} \in \Omega$ that is defined via spherical coordinates (γ, φ) on a unit sphere Ω , $\gamma = \cos \theta$, $\theta \in (0, \pi)$ is the polar angle, $\varphi \in (0, 2\pi)$ is azimuth.

Extinction coefficient $\Sigma_t(\mathbf{r})$ and scattering coefficient $\Sigma_S(\mathbf{r})$ depend only on spatial point \mathbf{r} , whereas scattering phase function $p(\mathbf{r}, \mathbf{\Omega} \cdot \mathbf{\Omega}')$ depends on the inner product $\mathbf{\Omega} \cdot \mathbf{\Omega}' = \gamma\gamma' + \sqrt{1-\gamma^2}\sqrt{1-(\gamma')^2}\cos(\varphi - \varphi')$ (scattering angle cosine) at each spatial point.

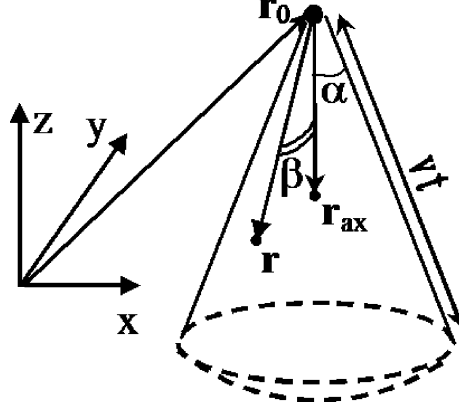
Value v is the speed of propagation of the radiation in the medium. Function $Q(\mathbf{r}, \mathbf{\Omega}, t)$ defines the intensity of the radiation source. A pulsed point source of small aperture α is under consideration, where angle α is measured from the axis $\mathbf{r}_{ax} - \mathbf{r}_0$, see fig. 1. In this case the function $Q(\mathbf{r}, \mathbf{\Omega}, t)$ should be defined via the generalized functions [1]

$$(1.2) \quad Q(\mathbf{r}, \mathbf{\Omega}, t) = S_0/[2\pi(1 - \cos \alpha)] \cdot \delta(\mathbf{r} - \mathbf{r}_0) \cdot \eta(C(\mathbf{r}) - \cos \alpha) \cdot \delta(t - t_0).$$

Here \mathbf{r}_0 is the source point coordinates, t_0 is the pulse emission time, S_0 is the source power $S_0 = \int_0^\infty dt \int d\mathbf{\Omega} \int d\mathbf{r} Q(\mathbf{r}, \mathbf{\Omega}, t)$; δ is Dirac's delta-function; $\eta(a)$ is Heaviside's function: $\eta(a) = 0$ as $a < 0$, $\eta(a) = 1$ as $a \geq 0$; $C(\mathbf{r}) = \cos \beta = \frac{\mathbf{r} - \mathbf{r}_0}{|\mathbf{r} - \mathbf{r}_0|} \cdot \frac{\mathbf{r}_{ax} - \mathbf{r}_0}{|\mathbf{r}_{ax} - \mathbf{r}_0|}$ is the cosine of the angle β between vectors $\mathbf{r} - \mathbf{r}_0$ and $\mathbf{r}_{ax} - \mathbf{r}_0$, see fig. 1. Zero boundary conditions are joint to eq. (1.1),

$$(1.3) \quad \Psi(\mathbf{r}, \mathbf{\Omega}, t) = 0, \quad \mathbf{r} \in \partial G, \quad \mathbf{\Omega} \cdot \mathbf{n}(\mathbf{r}) < 0.$$

Here $\mathbf{n}(\mathbf{r})$ is the outward normal to the boundary surface ∂G , and the condition (1.3) means that the radiation does not enter the region G across the surface ∂G at point \mathbf{r} .

Fig. 1. – Point source of aperture α .

Usually the phase function $p(\mathbf{r}, \boldsymbol{\Omega} \cdot \boldsymbol{\Omega}')$ is decomposed into the Legendre series

$$(1.4) \quad p(\mathbf{r}, \boldsymbol{\Omega} \cdot \boldsymbol{\Omega}') = \sum_{m=0}^{M(\mathbf{r})} (2m+1) p_m(\mathbf{r}) P_m(\boldsymbol{\Omega} \cdot \boldsymbol{\Omega}').$$

Here $M(\mathbf{r})$ is the expansion order, $p_m(\mathbf{r})$ are the expansion coefficients, $P_m(\boldsymbol{\Omega} \cdot \boldsymbol{\Omega}')$ are the Legendre polynomials. Addition theorem leads to the expansion of the scattering integral over spherical harmonics that are orthogonal on the unit sphere $\boldsymbol{\Omega}$

$$(1.5) \quad \hat{S}\Psi(\mathbf{r}, \boldsymbol{\Omega}, t) = \Sigma_S(\mathbf{r}) \sum_{m=0}^{M(\mathbf{r})} (2m+1) p_m(\mathbf{r}) \cdot \sum_{k=0}^m P_m^k(\gamma, \varphi) Y_{m,k}.$$

Here $P_m^k(\gamma, \varphi)$ are the spherical harmonics; $Y_{m,k}$ are the angular moments of the solution

$$(1.6) \quad Y_{m,k} = \int_{-1}^1 d\gamma' \int_0^{2\pi} d\varphi' P_m^k(\gamma', \varphi') \Psi(\mathbf{r}, \gamma', \varphi', t).$$

2. – Mesh algorithm

Because the singular source (1.3) cannot be approximated via mesh relations, analytical formulas should be applied to construct a numerical algorithm. The solution $\Psi(\mathbf{r}, \boldsymbol{\Omega}, t)$ is decomposed into three components that correspond to unscattered $\Phi_0(\mathbf{r}, \boldsymbol{\Omega}, t)$, single-scattered $\Phi_1(\mathbf{r}, \boldsymbol{\Omega}, t)$ and multiple-scattered $\Phi(\mathbf{r}, \boldsymbol{\Omega}, t)$ radiation intensities

$$(2.1) \quad \Psi(\mathbf{r}, \boldsymbol{\Omega}, t) = \Phi_0(\mathbf{r}, \boldsymbol{\Omega}, t) + \Phi_1(\mathbf{r}, \boldsymbol{\Omega}, t) + \Phi(\mathbf{r}, \boldsymbol{\Omega}, t).$$

Due to additivity of the radiative transfer equation, we now have to solve three linear problems:

for the unscattered radiation intensity $\Phi_0(\mathbf{r}, \boldsymbol{\Omega}, t)$

$$(2.2) \quad (1/v)\partial\Phi_0/\partial t + \hat{L}\Phi_0 = Q, \quad \Phi_0(\mathbf{r}, \boldsymbol{\Omega}, t)| = 0 \quad \text{as} \quad \boldsymbol{\Omega} \cdot \mathbf{n} < 0, \quad \mathbf{r} \in \partial G,$$

for the single-scattered radiation intensity $\Phi_1(\mathbf{r}, \mathbf{\Omega}, t)$

$$(2.3) \quad (1/v)\partial\Phi_1/\partial t + \hat{L}\Phi_1 = \hat{S}\Phi_0, \quad \Phi_1(\mathbf{r}, \mathbf{\Omega}, t)| = 0 \quad \text{as} \quad \mathbf{\Omega} \cdot \mathbf{n} < 0, \quad \mathbf{r} \in \partial G,$$

and for the multiple-scattered radiation intensity $\Phi(\mathbf{r}, \mathbf{\Omega}, t)$

$$(2.4) \quad (1/v)\partial\Phi/\partial t + \hat{L}\Phi = \hat{S}\Phi + \hat{S}\Phi_1, \quad \Phi(\mathbf{r}, \mathbf{\Omega}, t)| = 0 \quad \text{as} \quad \mathbf{\Omega} \cdot \mathbf{n} < 0, \quad \mathbf{r} \in \partial G.$$

The analytical solution of the problem (2.2) is found via the generalized function technique [1]

$$(2.5) \quad \Phi_0(\mathbf{r}, \mathbf{\Omega}, t) = S_0/[2\pi(1 - \cos \alpha)] \exp[-\tau(\mathbf{r}, \mathbf{r}_0)] \cdot \eta(C(\mathbf{r}) - \cos \alpha) \cdot w(\mathbf{r}, \mathbf{\Omega}, t),$$

where

$$w(\mathbf{r}, \mathbf{\Omega}, t) = \frac{1}{|\mathbf{r} - \mathbf{r}_0|^2} \delta(\mathbf{\Omega} - (\mathbf{r} - \mathbf{r}_0)/|\mathbf{r} - \mathbf{r}_0|) \cdot \delta(t - |\mathbf{r} - \mathbf{r}_0|/v),$$

$$\tau(\mathbf{r}, \mathbf{r}_0) = \int_0^{|\mathbf{r} - \mathbf{r}_0|} \Sigma_t(\mathbf{r}_0 + \xi \cdot \mathbf{\Omega}) d\xi.$$

Equation (2.5) means that the unscattered radiation propagates within the *radiation cone* $C(\mathbf{r}) \geq \cos \alpha$ (multiplier η) as a spherical wave with constant speed v (multiplier $w(\mathbf{r}, \mathbf{\Omega}, t)$), exponentially decaying along a trajectory (multiplier $\exp[-\tau(\mathbf{r}, \mathbf{r}_0)]$).

The unscattered radiation intensity forms the right side in eq. (2.3):

$$(2.6) \quad \hat{S}\Phi_0 = \frac{S_0}{2\pi(1 - \cos \alpha)} \frac{1}{|\mathbf{r} - \mathbf{r}_0|^2} \Sigma_S(\mathbf{r}, \xi) \exp[-\tau(\mathbf{r}, \mathbf{r}_0)] \eta(C(\mathbf{r}) - \cos \alpha) \delta(t - |\mathbf{r} - \mathbf{r}_0|/v),$$

where $\xi = (\mathbf{r} - \mathbf{r}_0) \cdot \mathbf{\Omega} / |\mathbf{r} - \mathbf{r}_0|$ is the cosine of the angle, at which the unscattered radiation at point \mathbf{r} must change its direction to take the direction $\mathbf{\Omega}$. In fact, the source (2.6) at time t is not zero only on the sphere $|\mathbf{r} - \mathbf{r}_0| = vt$, limited by the radiation cone $C(\mathbf{r}) \geq \cos \alpha$. These spatial points are designated by dashes in fig. 1.

The single-scattered radiation intensity $\Phi_1(\mathbf{r}, \mathbf{\Omega}, t)$ is found as an analytical solution to the problem (2.4), (2.6). It is non-zero only within the wave front

$$(2.7) \quad \Phi_1(\mathbf{r}, \mathbf{\Omega}, t)|_{\text{as } vt > |\mathbf{r} - \mathbf{r}_0|} = \frac{vS_0}{\pi(1 - \cos \alpha)} \cdot \exp[-\tau(\mathbf{r}', \mathbf{r})] \cdot \frac{\eta(C(\mathbf{r}') - \cos \alpha) \cdot \Sigma_S(\mathbf{r}', \cos \phi)}{(vt)^2 - 2vt \cdot ((\mathbf{r} - \mathbf{r}_0) \cdot \mathbf{\Omega}) + |\mathbf{r} - \mathbf{r}_0|^2},$$

$$\Phi_1(\mathbf{r}, \mathbf{\Omega}, t) = 0 \quad \text{as} \quad vt < |\mathbf{r} - \mathbf{r}_0|,$$

where $\cos \phi = (\mathbf{r}' - \mathbf{r}_0) \cdot \mathbf{\Omega} / |\mathbf{r}' - \mathbf{r}_0|$. At the wave front $|\mathbf{r} - \mathbf{r}_0| = vt$ the solution $\Phi_1(\mathbf{r}, \mathbf{\Omega}, t)$ is considered as undefined so in this case the denominator in (2.7) vanishes for all directions $\mathbf{\Omega}$.

In eqs. (2.7) \mathbf{r}' stands for a point, where the radiation undergoes a scattering event at time $t' < t$, the value

$$\tau(\mathbf{r}', \mathbf{r}) = \int_0^{|\mathbf{r}' - \mathbf{r}_0|} \Sigma_t \left(\mathbf{r}_0 + \xi' \frac{\mathbf{r}' - \mathbf{r}_0}{|\mathbf{r}' - \mathbf{r}_0|} \right) d\xi' + \int_0^{|\mathbf{r} - \mathbf{r}'|} \Sigma_t \left(\mathbf{r}' + \xi' \frac{\mathbf{r} - \mathbf{r}'}{|\mathbf{r} - \mathbf{r}'|} \right) d\xi'$$

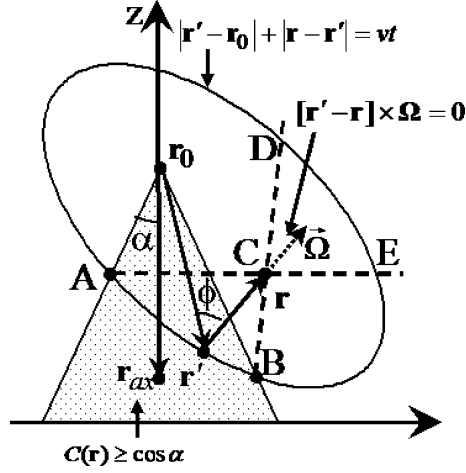


Fig. 2. – Path of radiation.

is the length (in mean free paths) of a trajectory from source \mathbf{r}_0 to the scattering point \mathbf{r}' then to the point \mathbf{r} , see fig. 2. Thus the exponential extinction of the single-scattered radiation intensity corresponds to the propagation of the radiation along the broken trajectory.

Change of the intensity $\Phi_1(\mathbf{r}, \boldsymbol{\Omega}, t)$ due to a scattering event is simulated in formula (2.7) by multiplier $\Sigma_S(\mathbf{r}', \cos \phi)$, where $\cos \phi$ is the cosine of the scattering angle, see fig. 2. Each scattering point \mathbf{r}' is uniquely defined via the point \mathbf{r} and the direction $\boldsymbol{\Omega}$. First, as the broken trajectory $(\mathbf{r}_0, \mathbf{r}', \mathbf{r})$ must be passed during time t , all points \mathbf{r}' obey the condition

$$(2.8) \quad |\mathbf{r}' - \mathbf{r}_0| + |\mathbf{r} - \mathbf{r}'| = vt.$$

Second, if the radiation propagates in the direction $\boldsymbol{\Omega}$ at the point \mathbf{r} , the scattering point \mathbf{r}' must be located on the ray

$$(2.9) \quad [\mathbf{r}' - \mathbf{r}] \times \boldsymbol{\Omega} = 0.$$

Intersection of the ellipsoid (2.8) and the ray (2.9) defines the unique point \mathbf{r}' at given \mathbf{r} and $\boldsymbol{\Omega}$. If this point \mathbf{r}' is out of the radiation cone, the $\Phi_1(\mathbf{r}, \boldsymbol{\Omega}, t) = 0$ (this condition is imposed by multiplier η in (2.7)). In other words, the single-scattered radiation intensity at given point \mathbf{r} and time t is not zero only in the directions $\boldsymbol{\Omega}$, those scattering points \mathbf{r}' are situated at the intersection between the ellipsoid (2.8) and the ray (2.9) within the radiation cone (surface AB in fig. 2). All these directions form the solid angle DCE.

According to the presentation (1.5), the right side of eq. (2.4) related to multiple-scattered radiation intensity $\Phi(\mathbf{r}, \boldsymbol{\Omega}, t)$ is entirely defined by the angular moments (1.6). They are approximated via the quadrature sums by the values $\Phi_1(\mathbf{r}, \boldsymbol{\Omega}, t)$, defined by eq. (2.7) in discrete directions $\boldsymbol{\Omega}_\ell$ that are introduced by uniform division of the solid angle DCE. Further, a mesh scheme of the discrete ordinate method and the successive-orders-of-scattering algorithm are used to solve the problem (2.4). The algorithm for accurate calculation of the angular moments (1.6), and their projections onto a spatial mesh, and the approximation of the non-stationary radiative transfer problem (2.4) are described in details in [2].

3. – Computations procedure

This algorithm is included into the code RADUGA-5.2(P) that has been developed to solve the transport equation in 1D, 2D and 3D geometries under weak restrictions on radiation sources and coefficients [3]. Our aim is to reduce the calculation time as much as possible. First of all the parallel algorithms should be used. The spatial decomposition method is applied, when at each iterative step a spatial subregion is calculated by a corresponding processor under known scattering integral and intensity of radiation, entering the subregion, from the preceding step. Data exchange among neighboring processors is performed after each iterative step. Widely spread MPI language is used to make the parallelization.

Most time is consumed to calculate the single scattered radiation intensity. Thus a supplementary acceleration of these calculations is in great demand. For instance, at a given time step some spatial subregions are out of wave front (for all spatial points $|\mathbf{r} - \mathbf{r}_0| > vt$) and the corresponding processors are free. Hence the additional parallelization is carried out, when all spatial cells, lying within the wave front, are uniformly distributed among all processors to parallel calculation of the single scattered radiation intensity. Further values, obtained by exterior processors, are sent to the corresponding interior ones.

Another acceleration technique is based upon flexible choice of the expansion order to the single scattered radiation intensity, see eq. (1.5). The farther is the point \mathbf{r} from the wave front, the lower number of angular moments (1.6) of the function $\Phi_1(\mathbf{r}, \mathbf{\Omega}, t)$ in the presentation (1.5) is required. Really, at given time step and spatial cell, the angular moments are put to zero, if they were negligibly small at the preceding time step.

The following reduction of the calculation time is done by replacing a conic source (1.2) by a corresponding mono-directional source:

$$Q(\mathbf{r}, \mathbf{\Omega}, t) = S_0 \cdot \delta(\mathbf{r} - \mathbf{r}_0) \cdot \delta(\mathbf{\Omega} - \mathbf{\Omega}_0) \cdot \delta(t - t_0).$$

The unscattered and single-scattered radiation intensity calculations in a monodirectional source problem are less time-consuming than similar calculations in a conic source problem. The source geometry can be disregarded only in cells far from wave front. So one of the two algorithms is applied at a spatial cell in dependence on the distance between the cell and the wave front.

4. – Numerical results

Let us consider the homogeneous medium with extinction coefficient $\Sigma_t = 9.4 \text{ mm}^{-1}$, scattering coefficient $\Sigma_s = 9.38 \text{ mm}^{-1}$, refractive index $n = 1.407575$. Let the phase function be Henyey-Greenstein with the mean cosine of the scattering angle $g = 0.900175$. These optical properties specify blood phantom with maximum physiological glucose concentration (500 mg/dl) interacting with infrared laser pulse. Let the radius and height of a cylindrical phantom be 10 mm and pulse source with aperture α of 14° be situated at the cylinder axis. Temporary distributions of the portion (%) of the diffuse radiation intensity reflected by the phantom and registered by the ring detector (limited by radii 0.15 mm and 0.3 mm) with aperture of 14° are of interest.

Calculations were performed using both the code RADUGA-5.2(P) [3] with the presented mesh method and the Monte Carlo code [4]. The phase function is represented by a sum of δ -function (peak) and P_{11} Legendre expansion (the rest component) via the

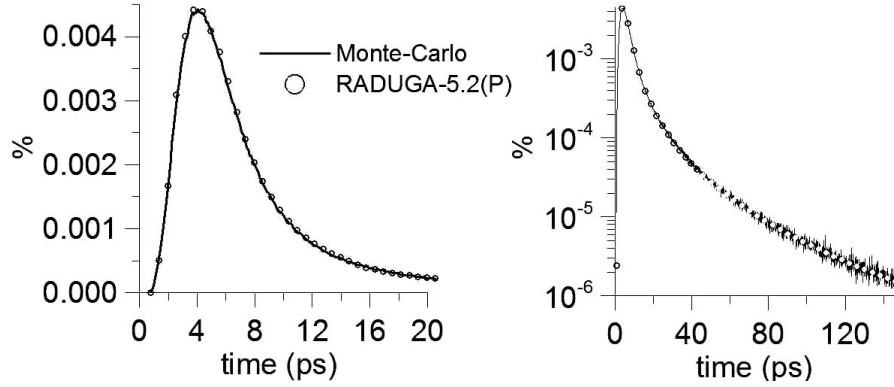


Fig. 3. – Temporal distributions of the detected diffuse radiation in the model problem.

Delta-M method [5] in the mesh method. Mesh method computations were run by 49 processors $2 \times$ AMD Opteron 248 (2.2 GHz) and took 25 minutes for one pulse calculation. Monte Carlo computations were run by 100 processors Intel Xeon (2.8 GHz) and took 10 min for one pulse calculation. So the time expenses of both methods are comparable.

Temporal distributions separately for a longer time interval (0–150 ps) and a shorter time interval (0–20 ps) are presented in fig. 3. One can see a good agreement of the results obtained by the statistical and the mesh methods if we neglect high stochastic noise, arising in Monte Carlo results for longer times of radiation propagation in the medium.

5. – Conclusion

New parallel mesh algorithm of the discrete ordinates method to simulate the propagation of ultrashort pulse of a point source of the small aperture in turbid media (for example, in biotissues) is presented. The algorithm is based upon the analytical expressions for unscattered and single-scattered radiation intensity and the mesh scheme to calculate the multiple-scattered radiation intensity. The algorithm includes a parallel technique (the spatial decomposition method) and different simplified approximations for both the source and the solution being sought to reduce the computation time.

The method is tested in the problem on infrared laser pulse propagation in blood phantom with elevated glucose concentration. The computation time is comparable to that required when using the Monte Carlo method. At the same time the solutions (temporary distributions of the intensity of diffuse radiation registered by a detector) obtained by both methods are close. However the mesh solution is not distorted by the stochastic noise that spoils the Monte Carlo solutions for larger times of signal propagation.

It can be concluded that potentially the developed mesh algorithm can be used to solve the inverse problems of light scattering from turbid media to substitute the Monte Carlo method.

* * *

LPB, OVN and VSK acknowledge the support by program N 3, project 3.2 of Mathematic Science Department of Russian Academy of Science. AVB and AVP acknowledge the partial support by RFBR grant 08-02-91760_af.

REFERENCES

- [1] GELFAND I. M. and SHILOV G. E., *Generalized Functions* (Academy Press, New York) 1968.
- [2] KUZNETSOV V. S., NIKOLAEVA O. V., BASS L. P., BYKOV A. V. and PRIEZZHEV A. V., *Mat. Model. [Math. Model.]*, **21** (2009) 3 (in Russian).
- [3] NIKOLAEVA O. V., BASS L. P., GERMOGENOVA T. A. and KUZNETSOV V. S., *Transp. Theory Stat. Phys.*, **36** (2007) 439.
- [4] BYKOV A. V., KIRILLIN M. YU. and PRIEZZHEV A. V., in *Handbook of Optical Sensing of Glucose in Biological Fluids and Tissues*, edited by VALERY V. TUCHIN (CRC Press) 2009, pp. 65-95.
- [5] WISCOMBE W. J., *J. Atmos. Sci.*, **34** (1977) 1408.